

Refinery Optimal Transitions by Iterative Linear Programming

Michael Mulholland*

University of KwaZulu-Natal, Department of Chemical Engineering, Durban, KwaZulu-Natal, South Africa

* Corresponding Author: mulholland@ukzn.ac.za

ABSTRACT

This paper focuses on the control and dynamics of an oil refinery process on an intermediate level - the flows, masses and compositions of and between units within the refining operation. It aims to elucidate optimal strategies for the routing of streams during upset events imposed on the process. A general flowsheet simulation technique including tunable controllers for flows, compositions, levels and reaction extents is incorporated in a Linear Programming model. A standard node represents a mixed receiving tank, with exit streams which can be split, converted and separated. These nodes can be inter-connected arbitrarily in the flowsheet. The method is demonstrated for the case of a planned 3-day shutdown of the catalytic cracker.

Keywords: flowsheet, control, horizon, profit, maximisation, constrained

1. INTRODUCTION

A number of authors report work on the optimization of the journey of “parcels” of crude oil through a refinery complex. Examples of this type of MILP/MINLP production planning (or “inventory planning”) are presented in the work of [1-4]. In [5], tank levels are tracked throughout, from crude supply to customer dispatch, allowing for service disruptions. In the work of [6], model predictive control is used up to a moving horizon, taking cognisance of the present status of crude parcel storage and processing, and anticipated deliveries. The approach in [7] was to use a genetic algorithm to optimize crude oil movements, allowing for uncertainty of tank availability.

The present work focuses instead on the actual control dynamics of the refining process, within and between the flowsheet units. Intermediate storages may be provided to ease startups and upsets, so the optimization becomes a type of supply-chain problem. The authors in [8] considered how the locations and sizes of intermediate storage could be economically optimized taking into account capital costs, operating costs and product specifications and values. Their refinery representation was based on data from [9] and [10]. The present work uses the same data to construct a linear programming model of the refinery, with the purpose of examining the sequence of dynamic changes and flow re-routings

required to maximise profitability during planned and unplanned upsets.

2. MODEL

With the aim of representing a range of process flowsheets, a systematic method of creating the linear programming equations was sought. This was based on a multi-purpose “node” consisting of a mixed storage tank which received inflows, with optional configurable reactors, separators and splitters on its outflows (Fig. 1). Here stream flows f , stream compositions x , tank compositions X , component masses m and tank masses M are used to define the mass balances. Such nodes could be interconnected arbitrarily, even allowing recycles.

In the basic mass balance, the compositions of the streams leaving the storage are expected to equate to the composition of the tank inventory, resulting in non-linear terms $f_j m_k / M_k$ in the mass balance. In the present work, this problem was dealt with using estimates of the tank compositions $X_k = m_k / M_k$ based on the previous solution of the linear program, and updating on each iteration until convergence. The inclusion of conversion, separation and stream splitting for multiple streams leaving a “tank” meant that final departing stream compositions x_j were ultimately fixed on the basis of the tank composition X_k , determined in the preceding LP solution.

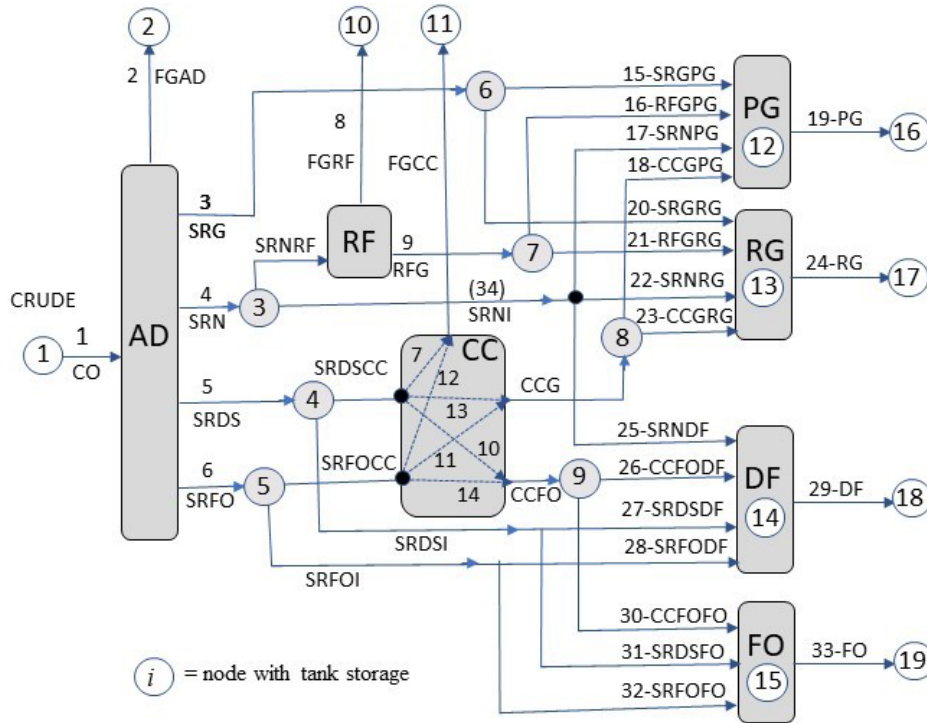


Figure 2: Simplified oil refinery flow diagram following [8]

Table 1: Economically optimal steady-state daily rates accounting for crude oil and product marginal values and associated processing costs, but excluding depreciation.

Stream [bbl/day]	Constraint	Optimal SS
1-CO Crude Oil	≤ 100000	(max) 100000
19-PG Premium Gasol.	≥ 23557	52645
24-RG Regular Gasol.	≥ 11260	21942
29-DF Diesel Fuel	≥ 8419	14058
33-FO Fuel Oil	≥ 2826	(min) 2826
(8,9) SRN to Reformer		(all) 23700
(7,10,13) 5-SRDS to CC		0
(12,11,14) 6-SRFO to CC		(all) 37200
(2,7,8,12) Total off-gas		8528
OCT-PG 19-PG octane	≥ 93	(min) 93.0
OCT-RG 24-RG octane	≥ 87	(min) 87.0
VP-PG 19-PG vap pres	≤ 12.7	8.88 mmHg
VP-RG 24-RG vap pres	≤ 12.7	11.97 mmHg
DENS-DF 29-DF density	≤ 306	293.3 lb/bbl
DENS-FO FO density	≤ 352	293.4 lb/bbl
SULPH-DF 29-DF sulphr	≤ 0.5	0.430 lb/bbl
SULPH-FO 33-FO sulphr	≤ 3.0	0.726 lb/bbl

Net profit / day (after material & operating costs, excluding capital depreciation) **1.918×10^6 \$/day**

Return on USED crude oil value **32.92%**
These create additional streams which, together

with direct streams from the crude distiller, are combined in various ways to achieve the requirements of four main product streams: Premium Gasoline, Regular Gasoline, Diesel Fuel and Fuel Oil (19-PG, 24-RG, 29-DF, 33-FO) which are drawn from the finished product tanks marked PG, RG, DF and FO. The PG and RG are required to exceed minimum octane levels, and to be below a maximum vapour pressure level. The DF and FO must be below maximum density and sulphur levels (Table 1).

Around the outside of the diagram are nodes 1,2,10,11 and 16-19 – which are accumulators representing a supplier (crude oil) and customers (off-gas, premium & regular gasoline, diesel, fuel oil) for accounting purposes. “Off-gas” here refers to the byproduct gas discarded from the distillation, reforming and catalytic cracking. The objective in a 20-day case study was to maximise the value of the total inventory of the plant – including the accumulators. The marginal values and processing costs are given in tables A1 and A4. The internal nodes in the process have level setpoints of 67%, representing 2 days of operation at optimal conditions. These will reveal which storage best contributes in the event of an upset. Level setpoint weights are sufficient to prevent internal inventory emptying out to more valuable product.

4. STEADY-STATE OPTIMAL OPERATION

- Table 1 and Fig. 4a: Operation is stretched between minimizing octane for PG and RG at the top end (to spread available octane as far as possible), and minimizing FO production at the bottom end (which is a loss against the crude oil value – see Table A1)
- Straight Run Diesel (SRDS) bypasses the Catalytic Cracker to make up the entire Fuel Oil output (FO), and part of the Diesel Fuel (DF), where the sulphur is diluted using cracked Fuel Oil
- Cracked Fuel Oil, with its moderate octane, also becomes a major contributor to PG and RG where it helps to lower vapour pressure.
- All Straight Run Naphtha is reformed to 104 octane and sent to PG

5. PLANNED 3-DAY SHUTDOWN OF THE CATALYTIC CRACKER

The plant is initially running at its steady-state economic optimum. With all setpoints satisfied, only the economic terms (marginal values Table A1 and processing costs Table A4) influence the objective function. A planned 3-day shutdown of the catalytic cracker starts on day 6, so some evasive actions start in the first 5 days of the simulation. These include pre-shutdown surges of CCG to the PG product (Fig. 3a), and of CCFO to the DF product, followed by similar brief recovery surges just after the shutdown. There are surges of the SRFO to both the DF (Fig. 3b) and FO (Fig. 3c) products near the end of the shutdown, with the FO product struggling to maintain its minimum flow by draining both its storage vessel 15 (Fig. 3d) and SRFO storage 5 (Fig. 3e). The surge in SRFO to the DF product causes the DF product to reach its maximum sulphur content briefly (Fig. 3f). Extra SRG re-routed from PG to the RG product (Fig. 3g) during the shutdown causes RG to briefly reach its maximum vapour pressure (Fig. 3h). Although the crude feed rate manages to remain steady at its maximum, production rates of PG (Fig. 3i) and DF (Fig. 3j) fluctuate, reaching their minima.

In Fig. 4a a visual impression is given of the sequence of events at times before and during the shutdown. In Fig. 4b storage of SRFO is being drained whilst catalytically cracked fractions are rapidly dispatched to PG in advance of the shutdown.

The average net profit per day (over the 20 days) decreases marginally from 1.918 to 1.914×10^6 \$/day, as a result of the shutdown. Likewise there is a slight decrease in the profit per barrel of crude oil used, from 32.92 to 32.84%. This remarkably small impact during a major upset is largely due to the use of the Straight Run Fuel Oil storage at node 5 during the transition (Fig. 3e). The case of an *unplanned* shutdown (not presented here)

is simulated with a shutdown start at steady-state on day 1, and shows similar but more radical recovery actions thereafter.

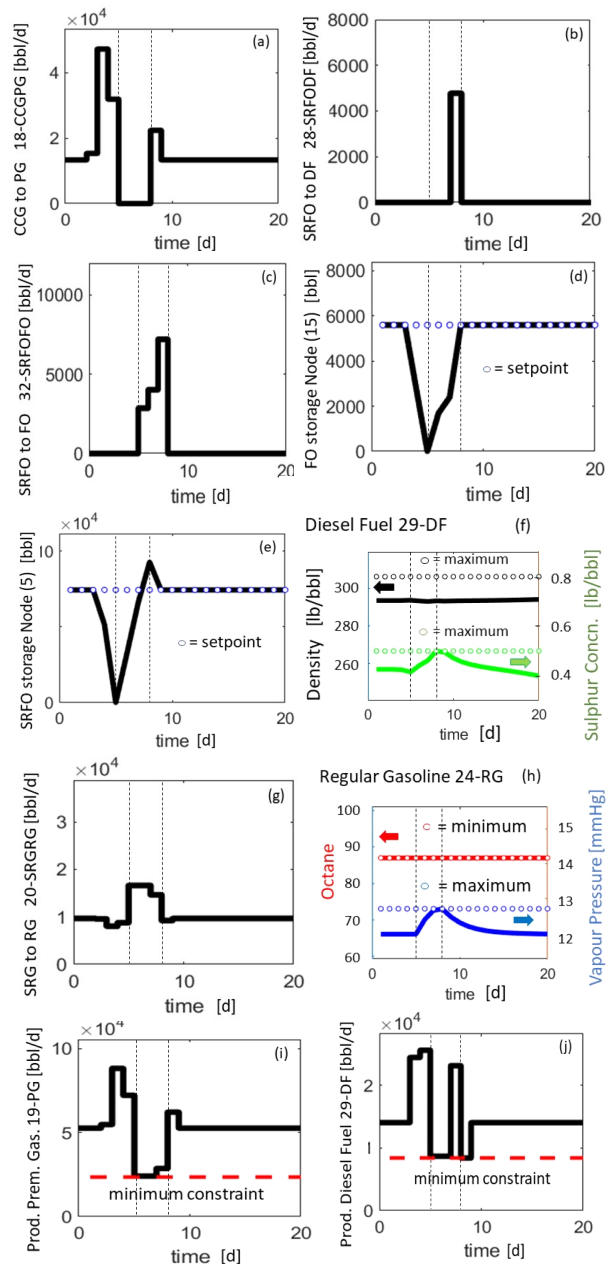
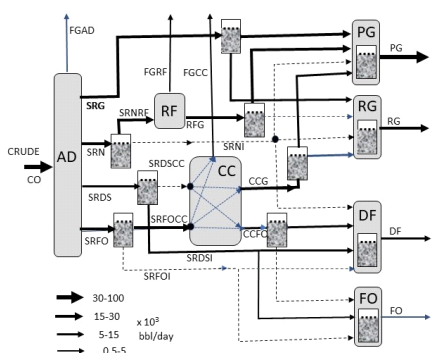


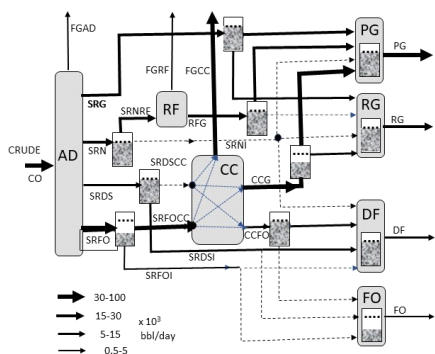
Figure 3. Planned 3-day shutdown of the catalytic cracker.

6. CONCLUSION

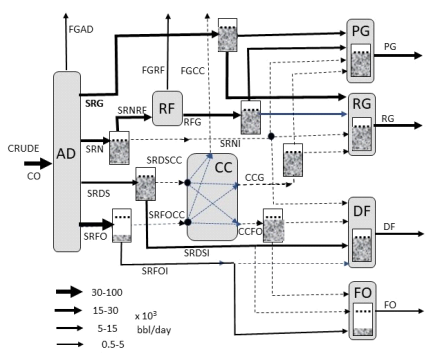
In this work a method is presented for dynamic optimisation of a process flowsheet, accounting for storage responses where necessary, and synchronizing transfers between units. The iteration of the LP solver provides an opportunity to update stream compositions, facilitating conversions, separations and stream splits.



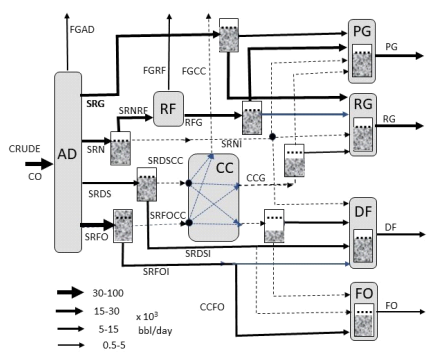
(a) Day 1: Optimal steady-state operation



(b) Day 4: 2 days before shutdown



(c) Day 6: Shutdown start



(d) Day 8: Mid-shutdown

Figure 4. Stream flows and storage during a 3-day planned shutdown of the catalytic cracker

The method is effective for dealing with the inherent non-linearity of the mass-balance, allowing use of the robust features of linear programming. Between LP solutions, stream compositions are calculated on the basis of the recent solution, and then frozen as fixed variables for the next LP solution. At convergence, the original non-linear mass balances are all satisfied. Instability is avoided by smoothing the composition update.

A feature of the work which eased the loading of the LP variables and equations was the idea of the standard node which could provide mixing, splitting, conversion and component separation based on specified fractions and desired reaction extents. Configured to represent the operating conditions of [8], as shown in Tables A2 and A3, the steady-state economic optimum operating point was found, and subjected to upsets such as a crude change, reformer shutdown, and catalytic cracker shutdown. As seen in the latter case presented here, the process is rapidly returned to its steady-state economic optimum operating point. The generous provisions of inter-unit storage served to reveal those storages which particularly helped minimize loss.

In this refinery simulation, the key free variables were obviously the flows f . Like all other free variables these were subject to range inequality constraints as noted in Table 1. Additionally, flows were subject to flow ratio equality constraints as detailed in Fig. 1, as well as rate-of-change ramp constraints. Other free variables were tank total masses M , compositions X and conversion extents ϵ . These variables could all be controlled to setpoints (though flow setpoints and composition setpoints were unweighted in this solution). So that requires two more free variables in each case – non-negative plus and minus deviations δp , δM from setpoint. The objective function penalised these deviations, rewarded tank inventory values, and penalised a similar absolute value of flow steps for move suppression.

In the present study all utilised setpoints were achievable at steady-state – therefore the steady-state yielded the economic optimum. One notes that the “optimality” of a transition requires prior knowledge of the future – eg. the length of a shutdown. Future work will consider placing the solution in an updated (“best guess”) predictive control loop.

With the above variables individually represented at each time over the simulation horizon (20 steps), the total number of free variables amounted to 7700. These were constrained by 2120 inequality equations and 5180 equality equations. All solutions converged within 9 iterations taking a maximum of 50 seconds. Programming was done in MATLAB under Windows 10 E with a PC specification: Core 17-10510U @ 1.80 GHz with 4 cores, 8 Logical Processors and 16 GB RAM.

APPENDIX

Table A1: Product and intermediate marginal values [8,10].

Node	US\$/bbl
1 (CRUDE)	58.38
2 (FGAD)*	20.83
10 (FGRF)*	20.83
11 (FGCC)*	20.83
13 & 17 (RG)	76.47
14 & 18 (DF)	78.36
15 & 19 (FO)	55.92
3-9#	58.38

* Off-gas marginal values estimated from available data

Nominal value of inventory

Table A2: Profiles of streams arriving at blenders [8,9].

Stream	Oct-ane	Vapour Press. [mmHg]	Density [lb/bbl]	Sulphur [lb/bbl]
15-SRPGP	78.5	18.40		
16-RFGPG	104.0	2.57		
17-SRNPG	65.0	6.54		
18-CCGPG	93.7	6.90		
20-SRGRG	78.5	18.40		
21-RFGRG	104.0	2.57		
22-SRNRG	65.0	6.54		
23-CCGRG	93.7	6.90		
25-SRNDF			272.0	0.283
26-CCFODF			294.4	0.353
27-SRDSDF			292.0	0.526
28-SRFODF			295.0	0.980
30-CCFOFO			294.4	0.353
31-SRDSFO			292.0	0.526
32-SRFOFO			295.0	0.980

Table A3: Reactor fractional product contributions [8,9].

Out-streams	In-streams		
	4-SRN(RF)	5-SRDS(CC)	5-SRFO(CC)
8-FGRF	0.072		
9-RFG	0.928		
7-FGCC		0.192	
12-FGCC			0.092
13-CCG		0.619	
11-CCG			0.688
10-CCFO		0.189	
14-CCFO			0.220

Table A4: Estimated processing costs [8,10].

Unit	Capacity [bbl/day]	Operating Cost [\$/bbl]
Crude Distillation AD	100000	1.00
Catalytic Reformer RF	25000	2.50

REFERENCES

- Pinto JM, Joly M, Moro LF. Planning and scheduling models for refinery operations. *Comput Chem Eng* 24(9):2259–2276 (2000)
- Joly M, Moro LF, Pinto JM. Planning and scheduling for petroleum refineries using mathematical programming. *Braz J Chem Eng* 19(2):207–228 (2002)
- Gao X, Jiang Y, Chen T, Huang D. Optimizing scheduling of refinery operations based on piecewise linear models. *Comput Chem Eng* 75:105–119 (2015)
- Xu J, Zhang S, Zhang J, Wang S, Xu Q. Simultaneous scheduling of front-end crude transfer and refinery processing. *Comput Chem Eng* 96:212–236 (2017)
- Pitty SS, Li W, Adhitya A, Srinivasan R, Karimi IA. Decision support for integrated refinery supply chains Part 1 - Dynamic simulation. *Comput Chem Eng* 32:2767–2786 (2008)
- Yuzgec U, Palazoglu A, Romagnoli JA. Refinery scheduling of crude oil unloading, storage and processing using a model predictive control strategy. *Comput Chem Eng* 34:1671–1686 (2010)
- Panda D, Bayu F, Ramteke M. Discrete time reactive scheduling of gasoline blending and product delivery in presence of demand and component uncertainties using graphical genetic algorithm. *Comput Chem Eng* 143:107100 (2020)
- Boucheikhchoukh A, Berger V, Swartz CLE, Deza A, Nguyen A, Jaffer S. Multiperiod refinery optimization for mitigating the impact of process unit shutdowns. *Comput Chem Eng* 164:107873 (2022)
- Pike RW. Optimization for Engineering Systems. Van Nostrand Reinhold (1986)
- US Energy Information Administration. November 2019 Monthly Energy Review Technical Report (2019)

© 2025 by the authors. Licensed to PSEcommunity.org and PSE Press. This is an open access article under the creative commons CC-BY-SA licensing terms. Credit must be given to creator and adaptations must be shared under the same terms. See <https://creativecommons.org/licenses/by-sa/4.0/>

